Measurement and calibration of the nucleus position and its cross-sectional area ratio to increase the accuracy of finite element analysis

Jingchi Li
Third Clinical Medical College of Nanjing University of Chinese Medicine
Zhipeng Xi
Third Clinical Medical College of Nanjing University of Chinese Medicine
Xiaoyu Zhang
Third Clinical Medical College of Nanjing University of Chinese Medicine
Shenglu Sun
Third Clinical Medical College of Nanjing University of Chinese Medicine
Lin Xie (xielin6508@163.com)
Jiangsu Province Hospital of Integration of Chinese and Western Medicine https://orcid.org/0000-0002-2538-347X
Yang Liu
Changzheng Hospital

Research article

Keywords: Model calibration, Finite element analysis, Cross-sectional area ratio, Relative position, Range of motions, Computational accuracy

Posted Date: March 25th, 2020

DOI: https://doi.org/10.21203/rs.2.16546/v2

Abstract

Background: As a widely used biomechanical research method, finite element analysis (FEA) is an important tool for investigating the pathogenesis of disc degenerative diseases and optimizing spine surgical methods. However, the definitions of the relative nucleus position and its cross-sectional area ratio do not conform to a uniform standard, thus affecting the accuracy (ACC) of the FEA. Hence, this study aimed to determine a precise definition of the relative nucleus position and its cross-sectional area ratio to increase the ACC of the following FEA studies.

Methods: The lumbar relative nucleus position and its cross-sectional area ratio were measured from magnetic resonance imaging data and then calibrated and validated via FEA. Imaging data from patients without disc degeneration were used. The L4-L5 nucleus and disc cross-sectional areas and the distances between the edges of the annulus and nucleus were measured; the ratios between these values were calculated as P1 and P2, respectively. The FEA model was constructed using these measured values, and the relative nucleus position was calibrated by estimating the differences in the range of motion (ROM) between the model, wherein the ligaments, facet joints and nucleus were suppressed, and that of an in vitro study. Then, the ACC was re-estimated in the model with all non-bony structures by comparing the ROM, the intradiscal pressure (IDP), the facet contact force (FCF) and the disc compression (DC) under different sizes and directions of moments magnitudes to validate the measured and calibrated indicators.

Results: The interobserver homogeneity was acceptable, and the measured P1 and P2 values were 1.22 and 38%, respectively. Furthermore, an ACC of up to 99% was attained for the model under flexion–extension conditions when the calibrated P1 value (1.62) was used, with a model validation of greater than 90% attained under al most all of the loading conditions considering the different indicators and moment magnitude s.

Conclusion: The measured and calibrated relative nucleus position and its cross-sectional area ratio increase the ACC of the FEA model and can therefore be used in subsequent studies.

Background

Biomechanical deterioration is a key trigger for lumbar disc degenerative diseases (DDDs) [1-5]. Therefore, optimized finite element analysis (FEA), which is a widely used biomechanical research method, is an ideal approach for the accurate investigation of DDD pathogenesis and treatments [6-15]. A series of model validation methods have been implemented by comparing the differences in the range of motion (ROM), which is a key index for lumbar motility and stability, between the FEA results and those from widely cited in vitro studies [7, 10, 11, 14-18]. The accuracy (ACC) of the FEA models has been improved via model calibrations that used annulus and bone structures [19, 20]. However, inaccurate definitions of the relative nucleus position and its cross-sectional area still negatively affect the computational ACC of FEA studies.

To clarify this issue, the anterior and posterior sides of the annulus can be approximated as two differently sized quadrangular annuli on a specific plane. The O point is set as the pivot point of the applied torque and M1 and M2 are the applied forward and backward torques (i.e., flexion and extension), respectively. R1 and R2 are the distances between the anterior and posterior parts perpendicular to the torque axis centre and edges of the nucleus, respectively. As shown in the central section of the disc sagittal plane (Fig. 1), changes in R1 and R2 originating from different nucleus positions and cross-sectional areas will induce changes in the ROM under the same M1 and M2. Furthermore, this change will extend to different sections if the force on the two-dimensional planar structure is extended to three-dimensional space.

However, such methods have not been defined consistently in previous FEA studies. For example, Tang et al modelled the centre of the nucleus as being slightly posterior to the centre of the disc, occupying 43% of the total disc volume [9]. **Schmidt et al modelled the centre of the nucleus as being 3.5 mm towards the posterior side, with a nucleus size that was approximately 44% of the total disc area [20]. The lumbar model of Akiah et al determined that the nucleus accounted for 33% of the disc volume [21], whereas this rate increased to 50% in the model of Ottardi et al [22].** Numerous FEA studies are available that do not address the issues addressed by the above-mentioned studies. Given that individual differences are inevitable among the discs in different models, the accurate definition of the relative nucleus position should be a ratio (such as a ratio of the anterior and posterior edges of the annulus to the relative nucleus edges) rather than an ambiguous description (e.g., ‘slightly posterior’) or a specific value (e.g., 3.5 mm).

Herein, we present an approach to accurately define such indicators in a uniform manner and increase the ACC of subsequent FEA studies. We first analysed magnetic resonance imaging (MRI) data of non-degenerative discs to measure the key indicators. We then constructed a 3D lumbar model to calibrate and validate our measured values. An extensive literature search indicated that no similar studies have been published to date.

Methods

MRI measurements of the indicators

Collection and measurement of MRI data

Three observers, two senior spine surgeons and a seasoned musculoskeletal radiologist reviewed the lumbar MRI (Discovery MR750 3.0T, GE Healthcare; Chicago, Illinois, USA) data collected in our hospital over the past three years. **MRI data from 43 subjects (average age of 25.6 ± 4.3 years) were included in the current study.** The L4-L5 disc was selected owing to its high incidence rate of DDD. T2-weighted imaging in the sagittal plane was selected to assess the grades of disc degeneration based on the work of Pfirrmann et al [23], with Grade I and II degeneration considered indicative of a normal disc and included in this study [24]. The MRI data were independently reviewed, and they were included in the analysis only when all observers confirmed that the disc was a normal disc. To avoid the influence of gender differences, only male MRI data were collected for the following FEA model based on the imaging

data from a 24-year-old male volunteer. The kappa statistic was used to analyse the included imaging data to ensure homogeneity in the interobserver classification.

The distances from the anterior and posterior edges of the annulus to the nucleus edges are set as D1 and D2, respectively. The cross-sectional areas of the nucleus and disc are set as A1 and A2, respectively. The ratios between the mean values of D1 and D2 and A1 and A2 are set as P1 and P2, respectively (Fig. 2). Cronbach's α reliability statistic was calculated to ensure the homogeneity of the measured values [25, 26].

Calibration and validation of the FEA model

Construction of the normal model

Bone structures from L1 to S1 were reconstructed on the basis of the high-resolution computed tomography (CT) imaging data and were used as templates for model construction [6, 8, 9, 12, 14]. Fitted curves were used in the drawing of smooth surfaces to replace irregular surfaces in the reconstructed model. In this process, different parts of the templates were layered, and the outlines in each layer were traced by separate fitted curves to smooth the irregular surfaces (Fig. 3). To be consistent with the segment selection via MRI, the bone structures of the L4-L5 segments were selected, and the corresponding non-bone structures were constructed with the fitted curves; the facet joint gap was set as 0.5 mm [6, 9, 13]. The centroid of the annulus outlines and the inferior surface of L4 were defined as the same point for the accurate placement of the annulus. Six different ligaments and a capsule of facet joints were constructed during the FEA preprocessing phase [11, 12, 18, 21, 27, 28] **(Fig. 4)**. The definition of the relative nucleus position and its cross-sectional area ratio were confirmed according to P1 and P2, and the outer contour of the nucleus was obtained using the same ratio reduction as that of the disc contour to ensure that the intervertebral disc and nucleus have the same central point, for easy adjustment during the calibration process.

Boundary and loading conditions

Completely identical boundary conditions were used in the model calibration and validation processes. Tetrahedral and hexahedral elements with different sizes were selected during mesh generation **(Fig. 4 and Table. 1)**, with smaller sizes (mesh refinement) being used in areas that experienced serious mesh distortion. The contact type of each surface, excluding facet cartilage, was defined as bounded, and the cartilage–cartilage contact was defined as frictionless [8, 9, 14, 18, 28, 29]**.** Six degrees of freedom were rigidly fixed under the inferior of L5, and moments were applied to the superior of L**4 [6, 12, 16, 21].**

Model calibration

The calibration process was accomplished by adjusting the value of P1, which is a relatively easy adjustment in the model construction process, estimating the ROMs under a moment of 10 Nm and flexion–extension conditions, and finally comparing our FEA model results to the results of a widely cited

in vitro study [19, 20]. The nucleus, ligaments and facet joints were suppressed during this process. **Fig. 6** and Table 1 show the calibration algorithm and list the material properties, respectively.

Model validation

The model was validated by evaluating the difference between different biomechanical indicators, including the ROM, the intradiscal pressure (IDP), the facet contact force (FCF) and the disc compression (DC) from the current FEA model (with nucleus, ligaments and facet joints) and those from the in vitro studies to determine if the two measured and calibrated factors reflected real biomechanical indicators under different loading conditions and to determine whether the calibrated FEA model can be used in subsequent studies [30-32].

Additionally, different loading conditions were used for the computation of different model validation indicators. The IDP and FCF were computed under 7.5 Nm moments, the ROM was computed under a 10 Nm moment with a 100 N compressive force and the DC was computed under 1200N compressive force. Notably, the compressive force was applied on the superior surface of L1 rather than L4 in the in vitro study [17, 30]. Hence, the transformation of the stress on the upper surface of L1 to L4 should undergo an orthogonal decomposition (Fig. 5).

Results

Homogeneity test

The kappa values for the interobserver disc degenerative classification were in the 0.67–0.77 range, and the Cronbach's α values for D1, D2, A1 and A2, all of which were measured by different observers, were greater than 0.95. These values indicated acceptable interobserver homogeneity (Table 2) [25, 26], with the P1 and P2 values then calculated from the measured values and used in the FEA model (P1=1.22; P2=38%).

Calibration of the relative nucleus position

The definition of ACC is shown in Fig. 6, with the sensitivity of the data adjustment tested prior to calibration. We found that the ACC under flexion–extension reached 99% when the P1 value was calibrated to 1.62. This value was confirmed and used during the model validation process (Table 3 and Fig. 7).

Model validation

The validated model was modified using the calibrated relative nucleus position. We found that the ACC of ROM was higher than 90% under all loading conditions, including flexion-extension, left-right lateral bending and left-right axial rotation, and was higher under the flexion–extension condition (Table 4 and Fig. 8) [30]. **The ACCs of the IDP the FCF and the DC were also higher than 90% under almost the loading conditions except for the right side of FCF under extension condition (Fig. 9) [31, 32]. In which, the value**

of ACC was 82.28% and the difference between our computational result and the average value from in-vitro study was still obviously less than one standard deviation [32].

Discussion

We explored several methods that defined the relative nucleus position and its cross-sectional area ratio, but there were still several issues with regard to our FEA models [9, 20, 21, 30, 33]. The data from previous studies could not be directly used in our model construction owing to individual differences and the lack of consistent standards. For example, the previously published nucleus position, wherein its centre was located 3.5 mm towards the posterior of the disc [20], yielded a D2 value of less than 2 mm, which is obviously less than the minimum value measured in our study. Furthermore, the application of this value to the models constructed using imaging data from short volunteers may result in an impossible situation wherein part of the nucleus lies outside the disc's boundary. The lack of consistent definition methods also leads to repeated attempts at model construction and validation. Finally, we can only define the relative nucleus position as being 'slightly posterior' to the centre of the disc, such that the lowest ACC of our model was lower than 70%, which needs to be improved further, even though the model validation process was verified in our previously published studies**.** Therefore, the calibration of the relative nucleus position and the investigation of a reliable ratio to define the above indicators are vital for improving the ACC of FEA, a widely used research method in the investigation of pathogenesis of DDD and optimization of spine surgical methods [6, 9, 13, 27, 33].

The reduced T2 signal in the MRI data is closely related to disc degeneration and is generally selected to measure such a pathological change [23, 34]. The homogeneity test is important for ensuring the ACC and credibility of the study, as it is based on subjective observer measurements [23, 35]. While the kappa values between observers 1 and 3 are excellent (>0.75), the rest are only acceptable (>0.6). Such a phenomenon may be attributed to the small sample size and strict inclusion criteria of this study. These two constraints highlight that the slight interobserver differences can lead to obvious variations in the kappa values. Furthermore, although there is a certain degree of difference between the measured and calibrated relative nucleus positions, the modelled ROMs that are constructed from the measured nucleus position are still quite similar to the values from the in vitro study, with excellent ACC values attained (94.97% under flexion and 96.24% under extension, Fig. 7). The model constructed from the measured values also simulates real biomechanical indicators, such that the model calibration process further improves the ACC values based on the MRI measurements.

Notably, the nucleus itself was supressed during the model calibration process in the current study, even though the measured and calibrated values were closely associated with the nucleus. This is because R1 and R2 have an important impact on both M1 and M2 and their resultant ROMs. **The variation in the ROMs is more likely due to the change in the approximately quadrangular annulus areas caused by the change of relative nucleus position and its cross-sectional area rather than the nucleus itself.** The nucleus, ligaments and facet joints were therefore suppressed during the model calibration to investigate this factor individually. The FEA study results indicated that the retrodisplacement of the nucleus

improved the ACC during the calibration process. Furthermore, the posterior structures overlapped in the model calibration under the extension condition. This phenomenon is not indicated by the computation error; rather, it is caused by the omitted contact types between the bone structures. Therefore, spatial positions are independently calculated when facet cartilages have been supressed (Fig. 7).

Notably, the nucleus itself was suppressed during the model calibration process in the current study, even though the measured and calibrated values were closely associated with the nucleus. This is because R1 and R2 have an important impact on both M1 and M2 and their resultant ROMs. The variation in the ROMs is more likely due to the change in the approximately quadrangular annulus areas caused by the change in the relative nucleus position and its cross-sectional area rather than the nucleus itself. The nucleus, ligaments and facet joints were therefore suppressed during the model calibration to investigate this factor individually. The FEA study results indicated that the retrodisplacement of the nucleus improved the ACC during the calibration process. Furthermore, the posterior structures overlapped in the model calibration under the extension condition. This phenomenon is not indicated by the computation error; rather, it is caused by the omitted contact types between the bone structures. Therefore, spatial positions are independently calculated when facet cartilage is suppressed (Fig. 7).

In this study, the nucleus positions before and after calibration clearly changed (Fig. 7). We hypothesized that this change may originate from changes in body positions. The MRI measurement was completed in the supine position, whereas the loading conditions in the biomechanical studies were based on the standing position. Considering that the position of a nucleus cannot be changed once it was determined in the model construction process and that MRI data can be obtained in only the supine position, we believe that this model calibration is an effective method to calibrate this difference caused by body position and improve the computational ACC.

Differences still exist between the ROMs in the current FEA study and the widely cited in vitro study [30]; these differences may be due to the suppressed structures on the ROMs, even though the measurement and calibration of the relative nucleus position and its cross-sectional area ratio increase the ACC. This defect may also affect the ACC because the ligament definition also lacks a standard method. **There are no published in vitro ROM values that have been computed from models with the ligaments, facet joints and nucleus removed and with intact bone structures under lateral bending and axial rotation conditions. Although the in vitro study reported by Prof. Heuer et al provided ROM data under bending and axial rotation conditions with ligaments, facet cartilage, and the nucleus removed [36], these data could not be used as references for our model validation because the vertebral arch was also excised and proven to be somewhat related to lumbar instability [36-38]. In other words, ROM from these models will be greater than those of intact posterior structures. Hence, we are unable to calibrate the FEA model under these loading conditions.** This defect can provide a good explanation for the lower ACC under lateral bending and axial rotation conditions.

Due to the issue that ROM predictions alone are insufficient to validate models for predicting mechanical contact parameters, as reported by Prof. Woldtvedt et al [39], multi-indicator model validation was

necessary to evaluate the credibility of the measured and calibrated factors. In addition, although 10 Nm moments were widely used in published finite element studies [9, 10, 13, 40], model validations under smaller moments were also necessary for the wider application of these measured and calibrated factors [15, 28, 31, 32, 36]. Hence, IDP and FCF under 7.5 Nm moments and DC under 1200N compressive force were computed as validation indicators.

In this process, it is also worth noting that we did not determine the value of FCF from an in vitro study of the L4-L5 segment; hence, FCF from a widely cited in vitro study of the L3-L4 segment was selected as the standard value for the validation of FCF [32]. Computational FCF results indicated that the L4-L5 segment was slightly larger than the in vitro values (Fig. 9), and this result was consistent with the report that the facet contact force gradually increased from the cranial to the caudal side [39]. Despite these defects, we still believe that the difference in the model validation is acceptable because the lowest ACC value computed in the current study (among the ROM, IDP and FCF) is greater than 90% under almost all of loading conditions. Therefore, the measured P2 and calibrated P1 values in our subsequent FEA studies can be used to increase ACC.

Additionally, the annulus material property was defined as a linear elastic rather than hyper-elastic composite material. The reason for this definition was that the objective of this study was to calibrate the proposed model, which can be used in our future studies related to disc degenerative diseases (DDDs). Many studies on this topic have been reported [10, 12, 13, 41], and the risk of annular tears has been reported as one of the most important risk factors of DDD [1, 42] . Currently, the evaluation of the risk of annular tears was accomplished by comparing the variations in different kinds of stress, such as shear stress and von Mises stress, in the annulus; indeed, this is an effective method that has been used in our previous study [43]. However, these studies were qualitative, not quantitative studies; in other words, the risk of annular tears increasing with the stress concentration on the annulus can be evaluated by this method, but to what extent or when it tears cannot be illustrated clearly.

To evaluate the risk of annular tears quantitatively, the evaluation of damage accumulation under cyclic loading can be seen as a credible method. However, the only study evaluating the risk of annular tears under cyclic loading was reported by Prof. Qasim et al. from the Rush University Medical Center used linear elastic material [24]. The current study is not an independent study but a study to improve the credibility of our subsequent studies. To evaluate the risk of annular tears by cyclic loading, we referred to the S-N curve of the annulus in the study reported by Prof. Qasim et al., and thus, the material properties used in the model calibration process should be consistent with those from his study. This is the most important factor in the selection of the annulus linear elastic material properties.

It is also important to note that defining the annulus as a linear elastic material was also very common in published studies [24, 43-45]. More significantly, the computational results of different biomechanical indicators, including the ROM, the IDP the FCF and the DC, in the model validation process show excellent ACC compared with the validated values from in vitro studies and finite element studies with an annulus defined as a hyper-elastic composite material under different sizes of moments [12, 39, 41]. Therefore, we

have reason to believe that the definition of a linear elastic annulus will not decrease the reliability of finite element analysis, which can be used for future studies.

The current study still faces some limitations. The ratio measurement of nucleus position is based on cross-sectional areas in a specific two-dimensional plane rather than the three-dimensional volume, such that the models do not capture differences in the lumbar lordotic angle. For example, obvious changes in the disc volume can be observed in the models with the same cross-sectional area ratio and different lordotic angles. Furthermore, the definition of the ligaments was accomplished based on our observer measurements and did not conform to a uniform standard, even though ligaments play a significant role in the maintenance of lumbar stability [6, 11, 29] and are a key index in ROMs. Therefore, the definition of **ligaments should** be investigated and calibrated in future studies to further develop more accurate FEA models.

Conclusion

The measured and calibrated relative nucleus position (P1=1.62) and its cross-sectional area ratio (P2=38%) could indeed increase the ACC of the FEA model in our study, and these values can therefore be used in subsequent studies concerning the investigation of the pathogeneses of DDD and optimization of spine surgical methods.

Abbreviations

ACC: accuracy

DC: disc compression

DDD: disc degenerative diseases

FCF: Facet contact force

FEA: finite element analysis

IDD: Intradiscal pressure

ROM: Range of motions.

Declarations

Ethics approval and consent to participate

Approval for this study was obtained from the ethics committees of Jiangsu Province Hospital on Integration of Chinese and Western Medicine (2019LWKY015).

Consent to publish

Not Applicable

Availability of data and materials

All the data of the manuscript are presented in the paper.

Competing interests

The authors declare that they have no competing interests.

Funding:

This study was funded by the Foundation for leading talent in traditional Chinese medicine of Jiangsu province (2018SLJ0210) and Key project of jiangsu province social development (BE2019765). The funds provided by the above projects are used for the polishing of English manuscripts in the mother tongue, the conference affairs and travel expenses of studying courses related to three-dimensional spinal modeling and finite element analysis and the publication charges of this manuscript.

Authors' contributions:

LX, YL and JCL contributed to the concept and design of the study. ZPX, SLS and LX measured the MRI data. XYZ and JCL contributed to the model reconstruction. YL and JCL performed the model calibration and data analysis. LX, YL and JCL wrote and checked the manuscript. All authors read and approved the final manuscript.

Acknowledgement:

We acknowledge MSC. Tian Tang for the collection of the MRI data.

Authors' Information

E-mail address:

Jingchi Li: lijingchi9405@163.com

Zhipeng Xi: xizhipeng@vip.126.com
Xiaoyu Zhang: zxiaoyu1993@foxmail.com

Shenglu Sun: sunsl113@126.com

Lin Xie: xielin6508@163.com

Yang Liu: liuyangspine@hotmail.com

Co-corresponding authors:

Lin Xie

Department of Spine Surgery,

Third Clinical Medical College of Nanjing University of Chinese Medicine

100th. Shizi Street, Nanjing, 210028, Jiangsu Province

P.R. China.

Tel. +86 025 52362080

Fax. +86 025 85502829

E-mail.xielin6508@163.com

Yang Liu

Department of Spine Surgery

Changzheng Hospital Affiliated to the Naval Medical University,

415th. Fengyang Road, Shanghai, 200003,

P.R. China.

Tel. +86 18621195867

Fax. +86 021 81886000

Email. Liuyangspine@hotmail.com

References

1. Adams MA, Roughley PJ: **What is intervertebral disc degeneration, and what causes it?** *Spine* 2006, **31**(18):2151-2161.

2. Adams MA, Freeman BJ, Morrison HP, Nelson IW, Dolan P: **Mechanical initiation of intervertebral disc degeneration**. *Spine* 2000, **25**(13):1625-1636.

3. Liang J, Dong Y, Hong Z: **Risk factors for predicting symptomatic adjacent segment degeneration requiring surgery in patients after posterior lumbar fusion**. *Journal of Orthopaedic Surgery Research* 2014, **9**(1):97.

4. Paul P, Garton HJ, Gala VC, Hoff JT, Mcgillicuddy JE: **Adjacent segment disease after lumbar or lumbosacral fusion: review of the literature**. *Spine* 2004, **29**(17):1938-1944.

5. Wang H, Ma L, Yang D, Wang T, Liu S, Yang S, Ding W: **Incidence and risk factors of adjacent segment disease following posterior decompression and instrumented fusion for degenerative lumbar disorders**. *Medicine* 2017, **96**(5):e6032.

6. Hsieh YY, Chen CH, Tsuang FY, Wu LC, Lin SC, Chiang CJ: **Removal of fixation construct could mitigate adjacent segment stress after lumbosacral fusion: A finite element analysis**. *Clinical Biomechanics* 2017, **43**(Complete):115.

7. Lv QB, Gao X, Pan XX, Jin HM, Lou XT, Li SM, Yan YZ, Wu CC, Lin Y, Ni WF *et al*: **Biomechanical properties of novel transpedicular transdiscal screw fixation with interbody arthrodesis technique in lumbar spine: A finite element study**. *J Orthop Translat* 2018, **15**:50-58.

8. Más Y, Gracia L, Ibarz E, Gabarre S, Peña D, Herrera A: **Finite element simulation and clinical follow-up of lumbar spine biomechanics with dynamic fixations**. *Plos One* 2017, **12**(11):e0188328.

9. Tang S, Rebholz BJ: **Does lumbar microdiscectomy affect adjacent segmental disc degeneration? A finite element study**. *Journal of Surgical Research* 2013, **182**(1):62-67.

10. Wen-Hsien C, Yi-Jie K, Shang-Chih L, Chih-Wei W, Shih-Hao C, Yeung-Jen C, Jiun-Ren HJS: **Comparison among load-, ROM-, and displacement-controlled methods used in the lumbosacral nonlinear finite-element analysis**. *Spine* 2013, **38**(5):276-285.

11. Zhu R, Niu WX, Zeng ZL, Tong JH, Zhen ZW, Zhou S, Yu Y, Cheng LM: **The effects of muscle weakness on degenerative spondylolisthesis: A finite element study**. *Clinical Biomechanics* 2017, **41**(1):34-38.

12. Kim HJ, Kang KT, Chun HJ, Lee CK, Chang BS, Jin SY: **The influence of intrinsic disc degeneration of the adjacent segments on its stress distribution after one-level lumbar fusion**. *European Spine Journal* 2015, **24**(4):827-837.

13. Chuang WH, Lin SC, Chen SH, Wang CW, Tsai WC, Chen YJ, Hwang JR: **Biomechanical effects of disc degeneration and hybrid fixation on the transition and adjacent lumbar segments: trade-off between junctional problem, motion preservation, and load protection**. *Spine* 2012, **37**(24):1488-1497.

14. Li J, Zhang X, Xu W, Xi Z, Xie L: **Reducing the extent of facetectomy may decrease morbidity in failed back surgery syndrome**. *BMC Musculoskelet Disord* 2019, **20**(1):369.

15. Ho-Joong K, Heoung-Jae C, Hwan-Mo L, Kyoung-Tak K, Choon-Ki L, Bong-Soon C, Jin S, Yeom: **The biomechanical influence of the facet joint orientation and the facet tropism in the lumbar spine**. *Spine Journal* 2013, **13**(10):1301-1308.

16. Dreischarf M, Zander T, Shiraziadl A, Puttlitz CM, Adam CJ, Chen CS, Goel VK, Kiapour A, Kim YH, Labus KM: **Comparison of eight published static finite element models of the intact lumbar spine: predictive power of models improves when combined together**. *J Biomech* 2014, **47**(8):1757-1766.

17. Renner SM, Natarajan RN, Patwardhan AG, Havey RM, Voronov LI, Guo BY, Andersson GBJ, An HS: **Novel model to analyze the effect of a large compressive follower pre-load on range of motions in a lumbar spine**. *J Biomech* 2007, **40**(6):1326-1332.

18. Matsukawa K, Yato Y, Imabayashi H, Hosogane N, Asazuma T, Chiba K: **Biomechanical evaluation of lumbar pedicle screws in spondylolytic vertebrae: comparison of fixation strength between the traditional trajectory and a cortical bone trajectory**. *J Neurosurg Spine* 2016, **24**(6):910-915.

19. Schmidt H, Heuer F, Drumm J, Klezl Z, Claes L, Wilke HJ: **Application of a calibration method provides more realistic results for a finite element model of a lumbar spinal segment**. *Clinical Biomechanics* 2007, **22**(4):377-384.

20. Schmidt H, Heuer F, Simon U, Kettler A, Rohlmann A, Claes L, Wilke HJ: **Application of a new calibration method for a three-dimensional finite element model of a human lumbar annulus fibrosus**. *Clinical Biomechanics* 2006, **21**(4):337-344.

21. Akiah MA, Tanaka M: **Biomechanical investigation on the influence of the regional material degeneration of an intervertebral disc in a lower lumbar spinal unit: A finite element study**. *Computers in Biology Medicine* 2018, **98**.

22. Ottardi C, Galbusera F, Luca A, Prosdocimo L, Sasso M, Brayda-Bruno M, Villa TJME, Physics: **Finite element analysis of the lumbar destabilization following pedicle subtraction osteotomy**. *Medical Engineering Physics* 2016, **38**(5):506-509.

23. Pfirrmann CW, Metzdorf A, ., Zanetti M, ., Hodler J, ., Boos N, . %J Spine: **Magnetic resonance classification of lumbar intervertebral disc degeneration**. *Spine* 2001, **26**(17):1873-1878.

24. Qasim M, Natarajan RN, An HS, Andersson GB: **Damage accumulation location under cyclic loading in the lumbar disc shifts from inner annulus lamellae to peripheral annulus with increasing disc degeneration**. *J Biomech* 2014, **47**(1):24-31.

25. Grønbaek K, Christensen PB, Hamilton-Dutoit S, Federspiel BH, Hage E, Jensen OJ, Vyberg M: **Interobserver variation in interpretation of serial liver biopsies from patients with chronic hepatitis C**. *J Viral Hepat* 2002, **9**(6):443-449.

26. Perazzo H, Fernandes FF, Soares JC, Fittipaldi J, Cardoso SW, Grinsztejn B, Veloso VG: **Learning curve and intra/interobserver agreement of transient elastography in chronic hepatitis C patients with or without HIV co-infection**. *Clin Res Hepatol Gastroenterol* 2016, **40**(1):73-82.

27. Buell TJ, Bess S, Xu M, Schwab FJ, Lafage V, Ames CP, Shaffrey CI, Smith JS: **Optimal tether configurations and preload tensioning to prevent proximal junctional kyphosis: a finite element analysis**. *J Neurosurg Spine* 2019:1-11.

28. Kang KT, Koh YG, Son J, Jin SY, Park JH, Kim HJ: **Biomechanical evaluation of pedicle screw fixation system in spinal adjacent levels using polyetheretherketone, carbon-fiber-reinforced polyetheretherketone, and traditional titanium as rod materials**. *Composites Part B Engineering* 2017:S1359836817302159.

29. Bermel EA, Barocas VH, Ellingson AM: **The role of the facet capsular ligament in providing spinal stability**. *Comput Methods Biomech Biomed Engin* 2018, **21**(13):712-721.

30. Panjabi MM, Oxland TR, Yamamoto I, Crisco JJ: **Mechanical behavior of the human lumbar and lumbosacral spine as shown by three-dimensional load-displacement curves**. *J Bone Joint Surg Am* 1994, **76**(3):413-424.

31. Schilling C, Krüger S, Grupp TM, Duda GN, Blömer W, Rohlmann A: **The effect of design parameters of dynamic pedicle screw systems on kinematics and load bearing: an in vitro study**. *European spine journal : official publication of the European Spine Society, the European Spinal Deformity Society, and the European Section of the Cervical Spine Research Society* 2011, **20**(2):297-307.

32. Wilson DC, Niosi CA, Zhu QA, Oxland TR, Wilson DR: **Accuracy and repeatability of a new method for measuring facet loads in the lumbar spine**. *J Biomech* 2006, **39**(2):348-353.

33. Li J, Xu W, Zhang X, Xi Z, Xie L: **Biomechanical role of osteoporosis affects the incidence of adjacent segment disease after percutaneous transforaminal endoscopic discectomy**. *Journal of Orthopaedic Surgery and Research* 2019.

34. Modic MT, Masaryk TJ, Ross JS, Carter JR, %J Radiology: **Imaging of degenerative disk disease**. *Radiology* 1988, **168**(1):177-186.

35. Coste J, Judet O, Barre O, Siaud JR, Lara ACD, Paolaggi JBJJoCE: **Inter- and intraobserver variability in the interpretation of computed tomography of the lumbar spine**. *Journal of Clinical Epidemiology* 1994, **47**(4):375.

36. Heuer F, Schmidt H, Klezl Z, Claes L, Wilke H-J: **Stepwise reduction of functional spinal structures increase range of motion and change lordosis angle**. *J Biomech* 2007, **40**(2):271-280.

37. Mochida J, Nishimura K, Nomura T, Toh E, Chiba M: **The importance of preserving disc structure in surgical approaches to lumbar disc herniation**. *Spine* 1996, **21**(13):1556-1564.

38. Schaller B: **Failed back surgery syndrome: the role of symptomatic segmental single-level instability after lumbar microdiscectomy**. *European spine journal : official publication of the European Spine Society, the European Spinal Deformity Society, and the European Section of the Cervical Spine Research Society* 2004, **13**(3):193-198.

39. Woldtvedt DJ, Womack W, Gadomski BC, Schuldt D, Puttlitz CM: **Finite element lumbar spine facet contact parameter predictions are affected by the cartilage thickness distribution and initial joint gap size**. *J Biomech Eng* 2011, **133**(6):061009-061009.

40. Park WM, Kim K, Kim YH: **Effects of degenerated intervertebral discs on intersegmental rotations, intradiscal pressures, and facet joint forces of the whole lumbar spine**. *Comput Biol Med* 2013, **43**(9):1234-1240.

41. Ho-Joong K, Kyoung-Tak K, Juhyun S, Choon-Ki L, Bong-Soon C, Jin S, Yeom: **The influence of facet joint orientation and tropism on the stress at the adjacent segment after lumbar fusion surgery: a biomechanical analysis**. *Spine Journal Official Journal of the North American Spine Society* 2015, **15**(8):1841-1847.

42. Adams MA, Dolan P: **Intervertebral disc degeneration: evidence for two distinct phenotypes**. *J Anat* 2012, **221**(6):497-506.

43. Li J, Xu W, Jiang Q, Xi Z, Zhang X, Wang N, Xie L, Liu Y: **Indications Selection for Surgeons Training in the Translaminar Percutaneous Endoscopic Discectomy Based on Finite Element Analysis**. *BioMed Research International* 2020, **2020**:1-13.

44. Yang P, Zhang Y, Ding HW, Liu J, Ye LQ, Xiao J, Tu Q, Yang T, Wang F, Sun GG: **Pedicle screw fixation with kyphoplasty decreases the fracture risk of the treated and adjacent non-treated vertebral bodies: a finite element analysis**. *J Huazhong Univ Sci Technolog Med Sci* 2016, **36**(6):887-894.

45. Zhang L, Yang G, Wu L, Yu B: **The biomechanical effects of osteoporosis vertebral augmentation with cancellous bone granules or bone cement on treated and adjacent non-treated vertebral bodies: a finite element evaluation**. *Clin Biomech (Bristol, Avon)* 2010, **25**(2):166-172.

Tables

Table. 1 Material properties in the average radius calibrating model

	Young's modules (Mpa)		Possion ratio	Cross-sectional areas (mm2)	Element types	Element sizes (mm)
Cortical	12000		0.3	/	Tetrahedral	2.8
Cancellous	100		0.2	/	Hexahedral	3.5
Posterior structures	3500		0.25	/	Tetrahedral	4
Endplates	1000		0.4	/	Tetrahedral	1.2
Cartilages	10		0.4	/	Tetrahedral	0.45
Annulus	4.2		0.1	/	Tetrahedral	0.3
Nucleus	1		0.499	/	Tetrahedral	3.0
Capsules	7.5(<25%)	33(>25%)	0.3	30	Cable	/
ALL	8(<12%)	21(>12%)	0.3	60	Cable	/
PLL	11(<11%)	22(>11%)	0.3	21	Cable	/
LF	15(<6.2%)	19(>6.2%)	0.3	60	Cable	/
ITL	10(<18%)	59(>18%)	0.3	10	Cable	/
ISL	10(<14%)	12(>14%)	0.3	40	Cable	/
SSL	9(<20%)	16(<20%)	0.3	30	Cable	/

Abbrevation: Anterior longitudinal ligament (ALL), Posterior longitudinal ligament (PLL), Ligamentum flavum (LF), Intertransverse ligament (ITL), Interspinous ligament (ISL), Supraspinous ligament (SSL).

Table. 2 Homogeneity test of measured values

	Average values	Cronbach's α	Observers	Kappa values
D1	8.87 ± 1.51	0.97		
D2	7.29 ± 1.37	0.96	1&2	0.72
A1	1761.0 ± 206.1	0.96	2&3	0.77
A2	671.4 ± 123.8	0.98	1&3	0.67

1,2 and 3 stand for three observers in this study, 1 and 2 are senior spine surgeons and 3 is the musculoskeletal radiologist.

Table. 3 Calibration of nucleus relative position

ıdavers study (10 Nm)	P1	calibration data (°)	ACC (%)
Flexion (16.71°)	1.12	15.49	92.69
	1.22	15.87	94.97
	1.32	16.13	96.53
	1.42	16.31	97.61
	1.52	16.42	98.26
	1.62	16.55	99.04
Extension (-16.24°)	1.12	-17.12	94.58
	1.22	-16.85	96.24
	1.32	-16.51	98.34
	1.42	-16.39	99.08
	1.52	-16.30	99.63
	1.62	-16.21	99.82

Table. 4 Model validation in different loading conditons

FEA study (100N+10Nm)	F-E (°)	L-R B (°)	L-R A (°)
In-vitro study	12.66	10.01	2.19
This FEA study	12.70	9.46	2.38
ACC (%)	99.68	94.51	91.32

F-E: Flexion and extension, L-R B: Left and right lateral bending, L-R A: Left and right axial rotation

Figures

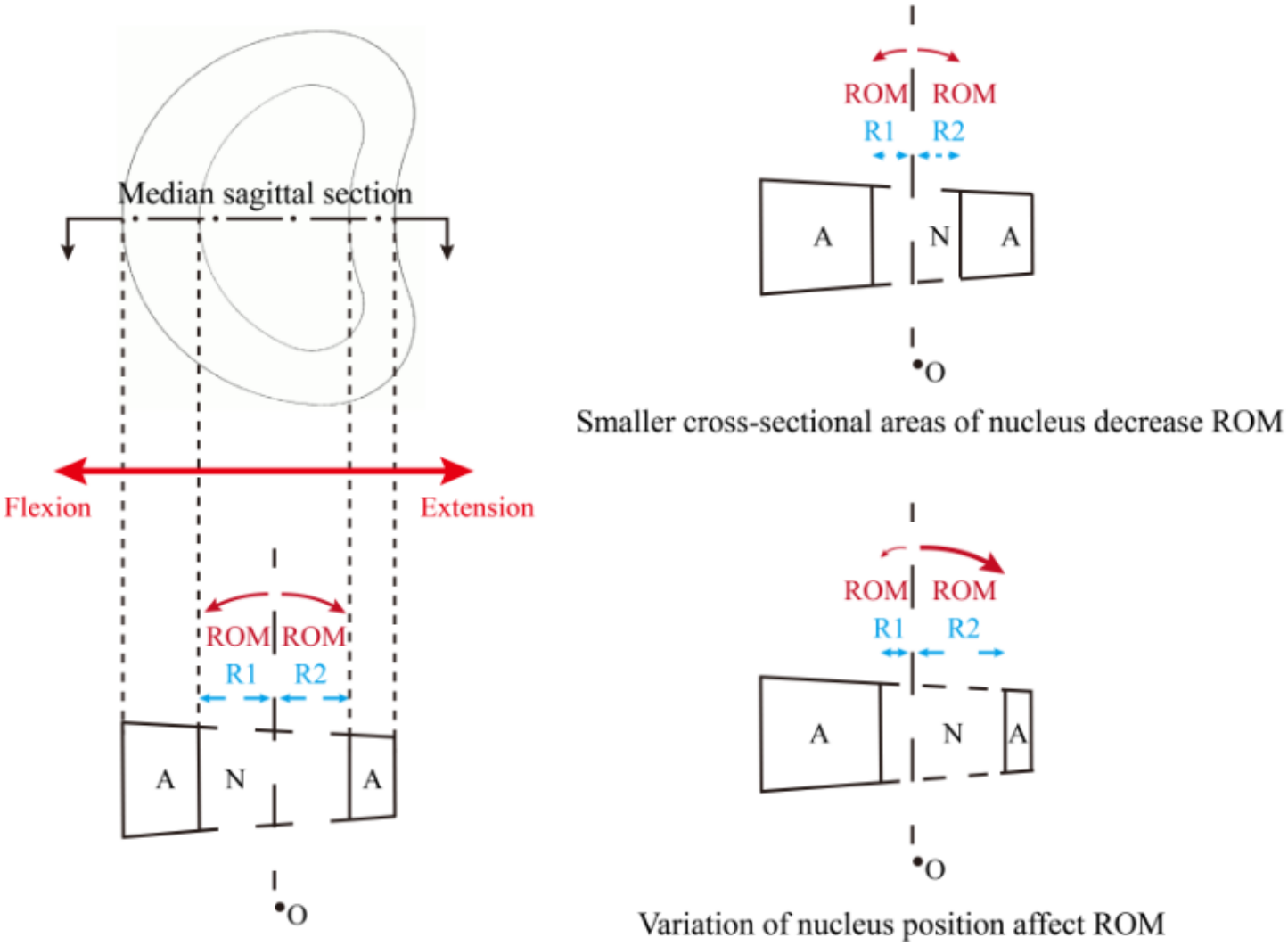

Figure 1

Effects of the variations in the nucleus cross-sectional areas and relative positions on the ROMs.

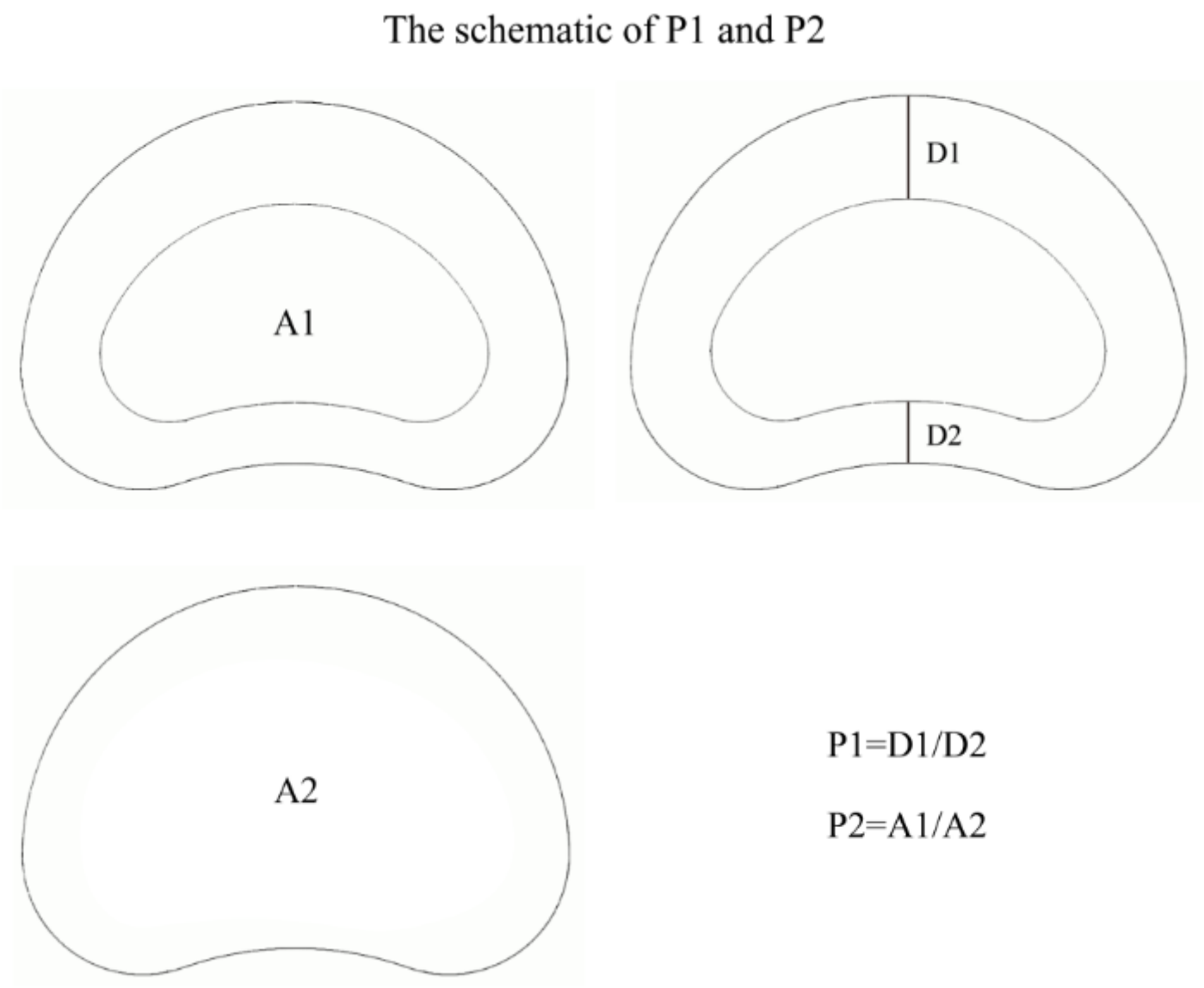

Figure 2

Schematic of P1 and P2

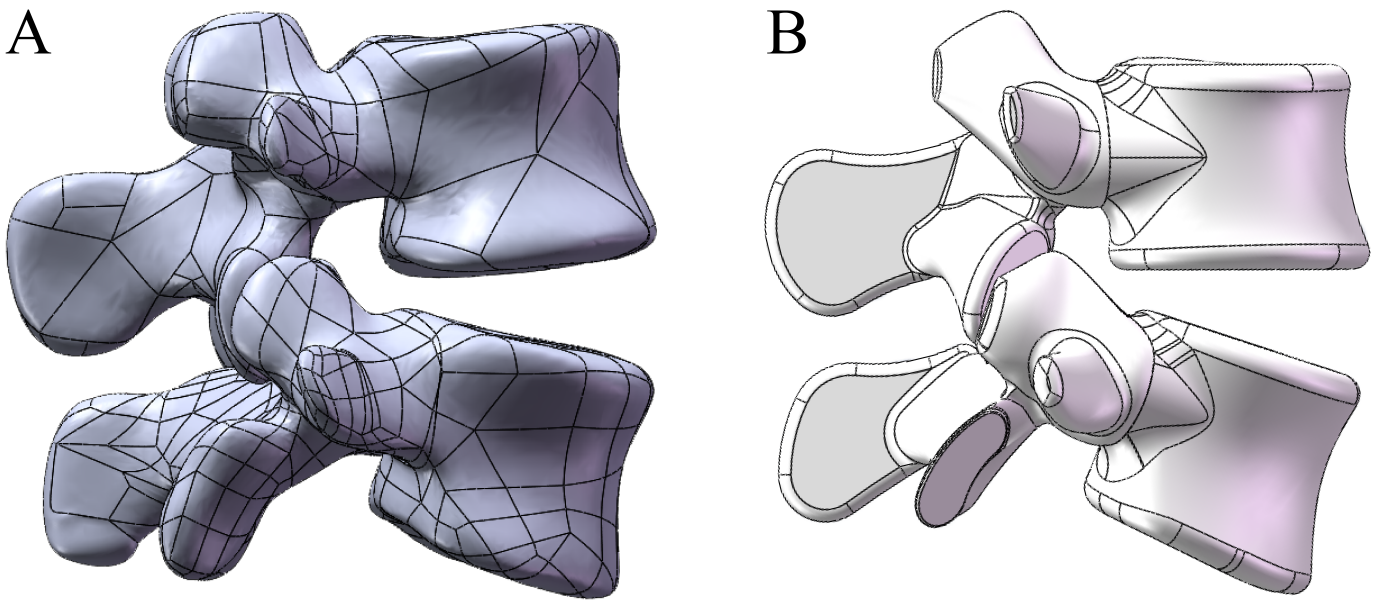

Figure 3

The construction of bone structures by fitted curves to smooth the irregular surfaces

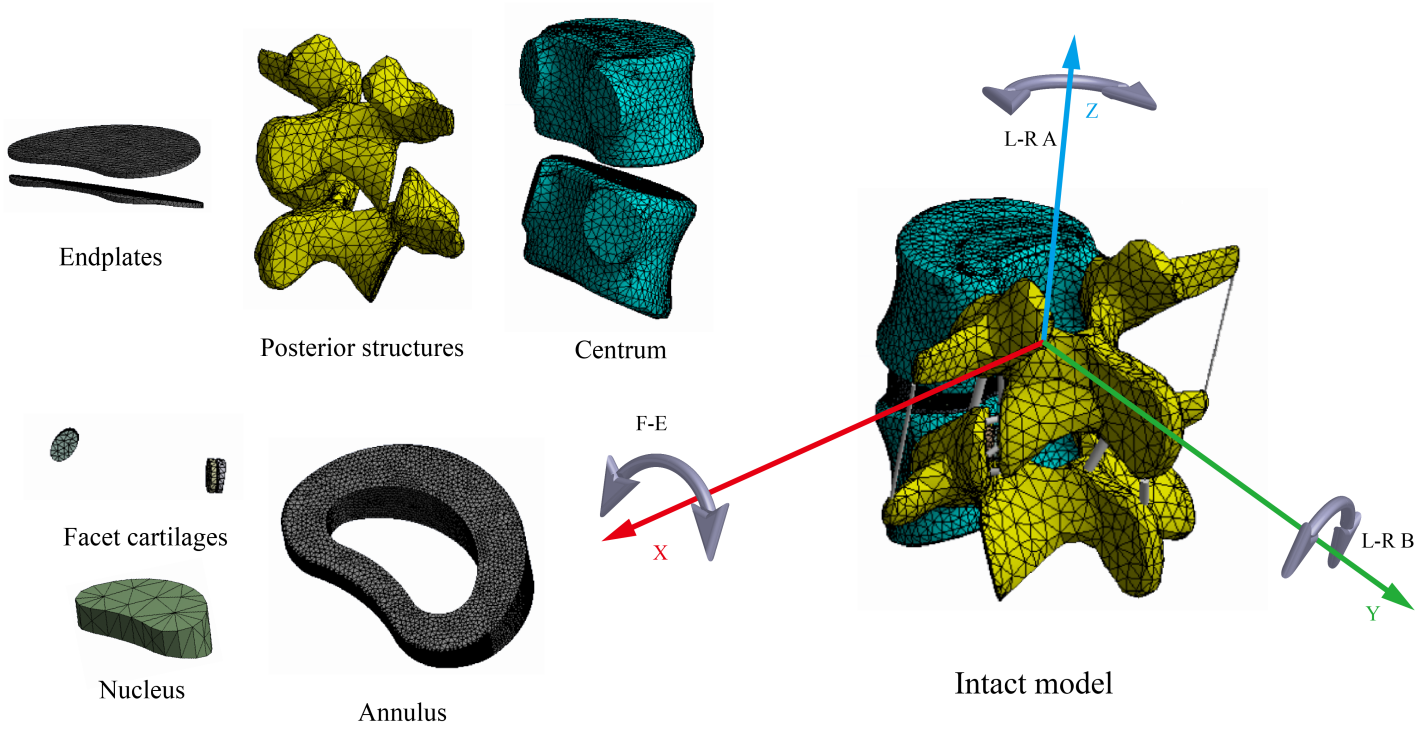

Figure 4

Intact model and components of the current models

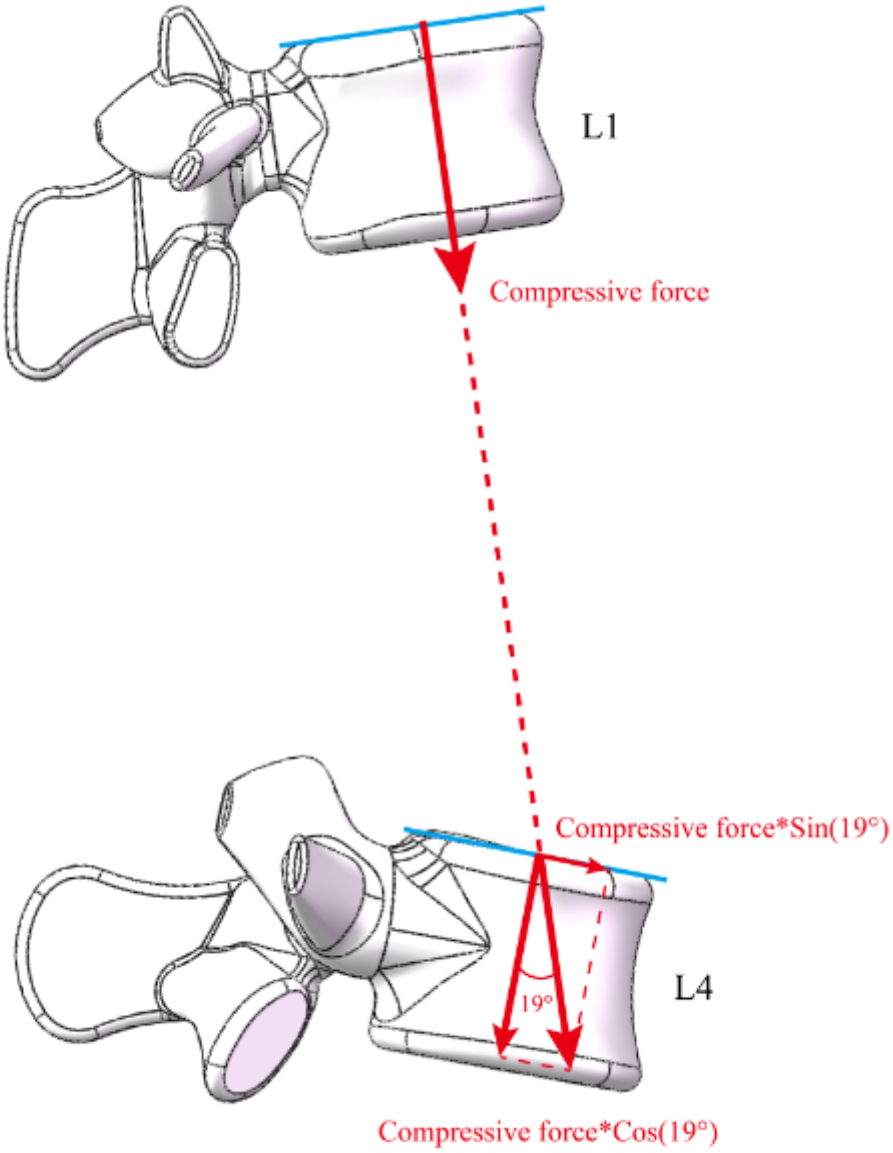

Figure 5

Schematic of the compressive force transfer

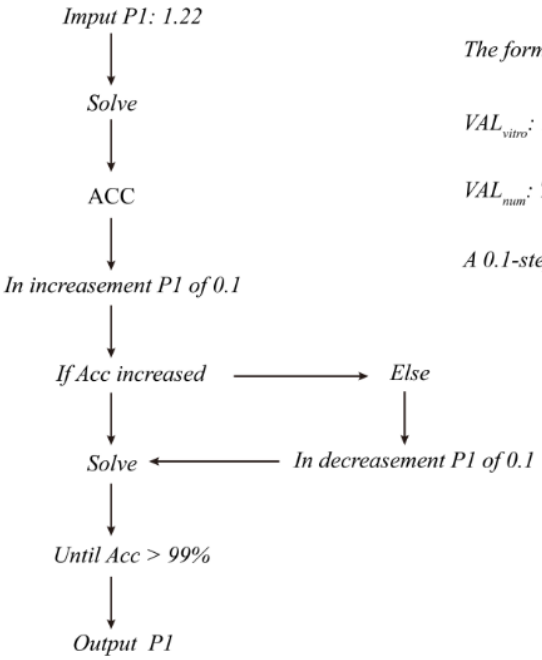

Figure 6

Calibration algorithm for the relative nucleus position.

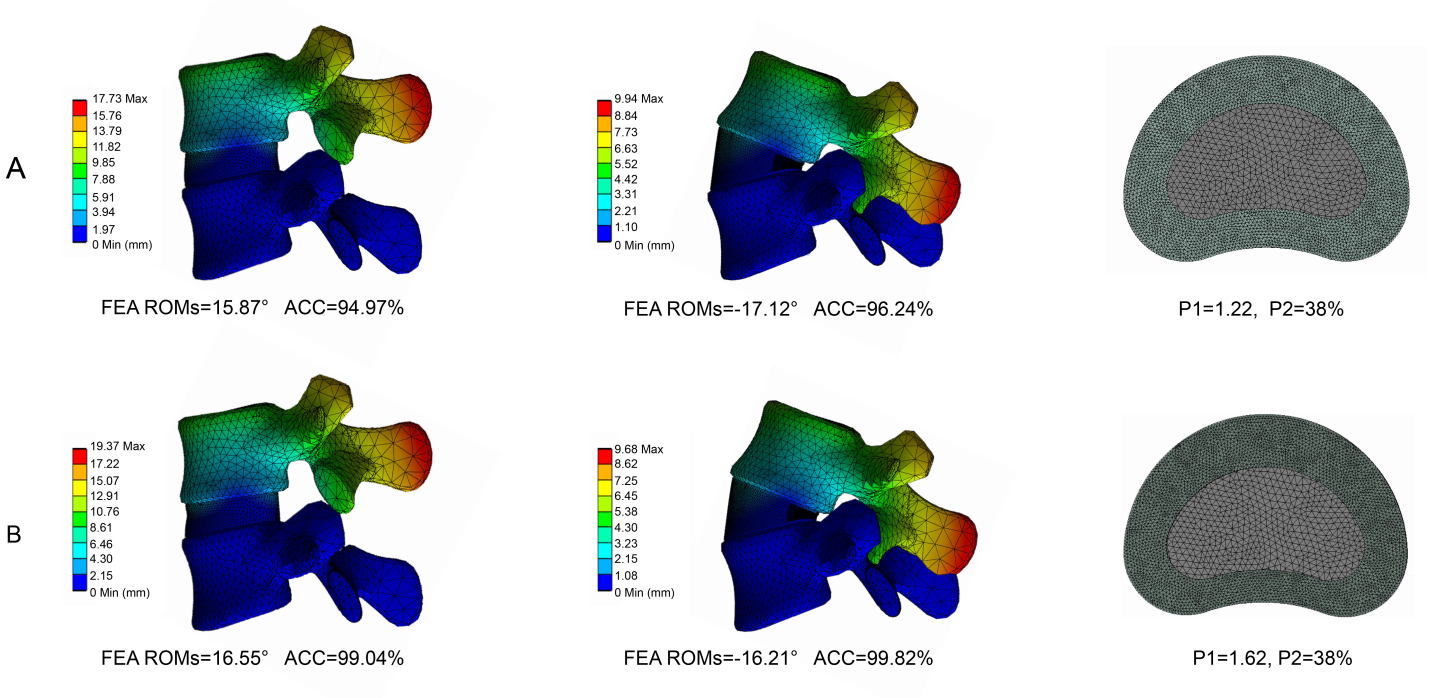

Figure 7

Variations in the ROMs before and after model calibration A. ROMs before the calibration of the relative nucleus position. B. ROMs after calibration of the relative nucleus position.

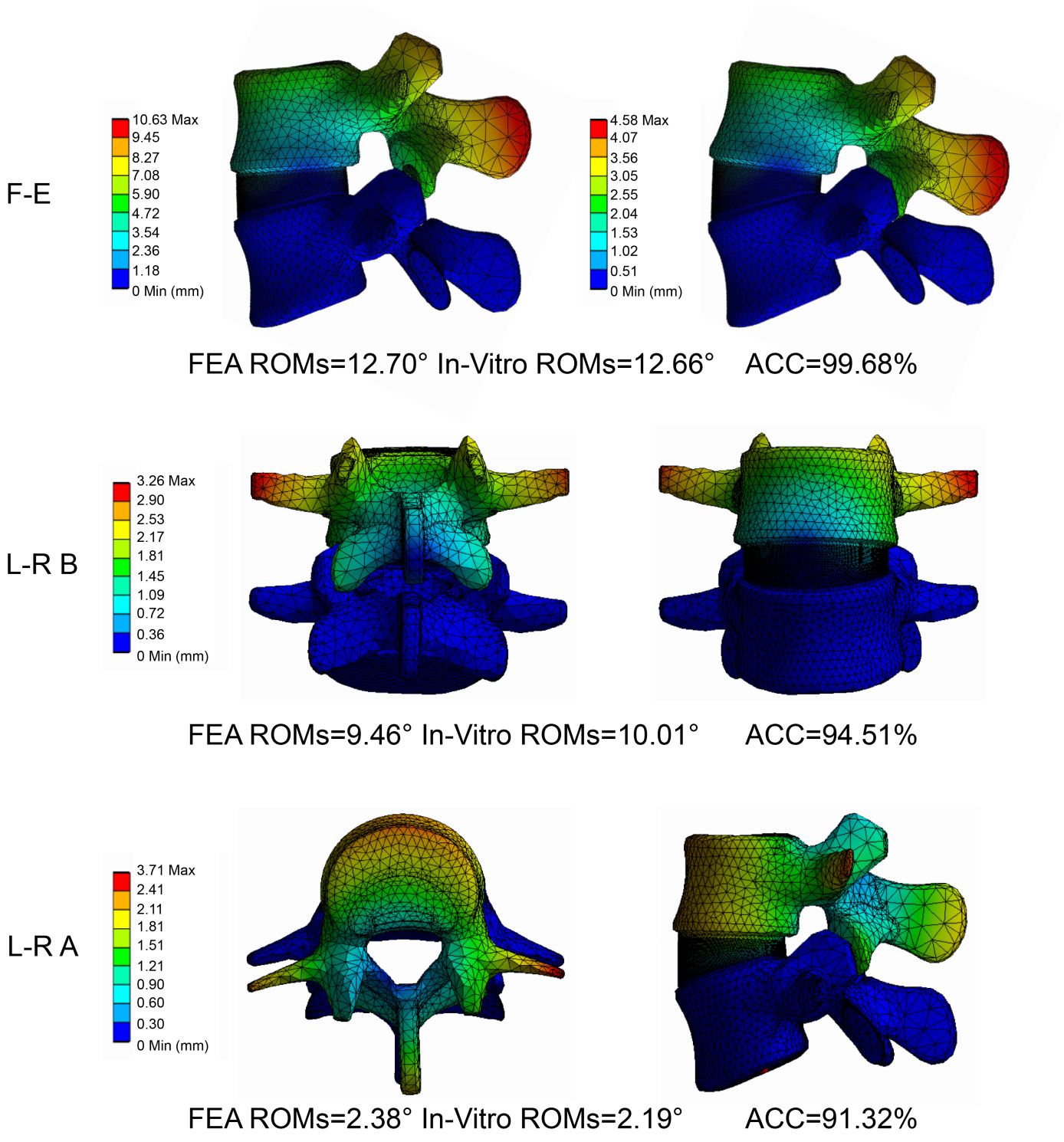

Figure 8

Validation of the calibrated model by comparing the ROM results F-E. Flexion-extension L-R B. Left-right bending L-R A. Left-right axial rotation

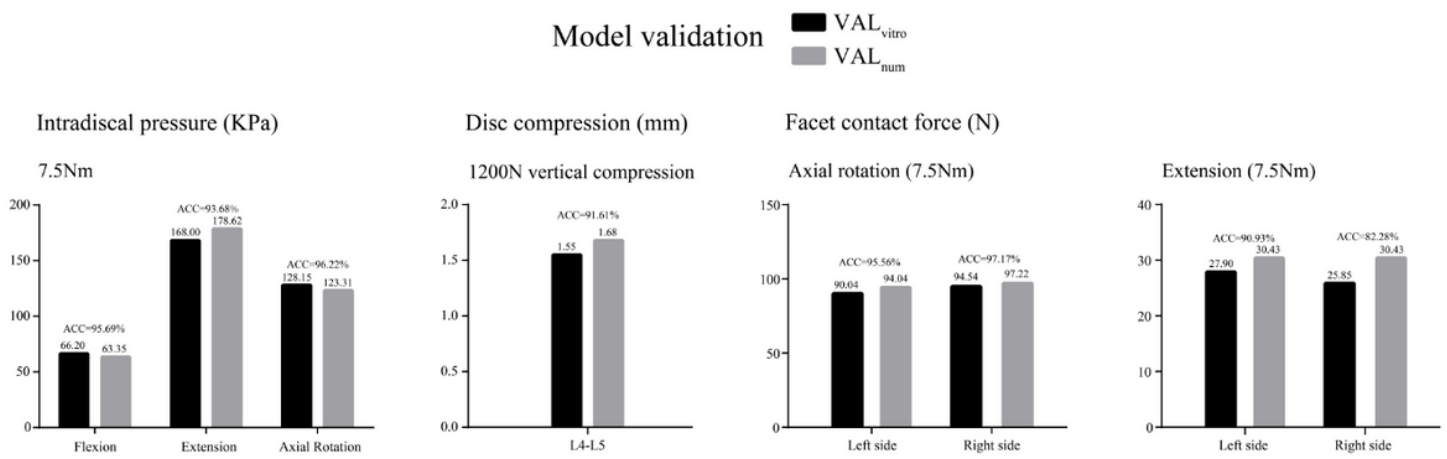

Figure 9

Validation of the calibrated model by comparing the IDP, FCF and DC results

Supplementary Files

This is a list of supplementary files associated with this preprint. Click to download.

- KeyPoints.docx